British Journal of Pharmacology (2008) 154, 774–786

0007–1188/08 $30.00
www.brjpharmacol.org

RESEARCH PAPER

Effects of MiRP1 and DPP6 β-subunits on the blockade induced by flecainide of K_V4.3/KChIP2 channels

S Radicke[1,2,3], M Vaquero[1,3], R Caballero[1], R Gómez[1], L Núñez[1], J Tamargo[1], U Ravens[2], E Wettwer[2] and E Delpón[1]

[1]*Department of Pharmacology, School of Medicine, Universidad Complutense de Madrid, Madrid, Spain and* [2]*Department of Pharmacology and Toxicology, Medical Faculty, Dresden University of Technology, Dresden, Germany*

Background and purpose: The human cardiac transient outward potassium current (I_{to}) is believed to be composed of the pore-forming K_V4.3 α-subunit, coassembled with modulatory β-subunits as KChIP2, MiRP1 and DPP6 proteins. β-Subunits can alter the pharmacological response of I_{to}; therefore, we analysed the effects of flecainide on K_V4.3/KChIP2 channels coassembled with MiRP1 and/or DPP6 β-subunits.
Experimental approach: Currents were recorded in Chinese hamster ovary cells stably expressing K_V4.3/KChIP2 channels, and transiently transfected with either MiRP1, DPP6 or both, using the whole-cell patch-clamp technique.
Key results: In control conditions, K_V4.3/KChIP2/MiRP1 channels exhibited the slowest activation and inactivation kinetics and showed an 'overshoot' in the time course of recovery from inactivation. The midpoint values (V_h) of the activation and inactivation curves for K_V4.3/KChIP2/DPP6 and K_V4.3/KChIP2/MiRP1/DPP6 channels were ≈10 mV more negative than V_h values for K_V4.3/KChIP2 and K_V4.3/KChIP2/MiRP1 channels. Flecainide (0.1–100 μM) produced a similar concentration-dependent blockade of total integrated current flow (IC_{50} ≈10 μM) in all the channel complexes. However, the IC_{50} values for peak current amplitude and inactivated channel block were significantly different. Flecainide shifted the V_h values of both the activation and inactivation curves to more negative potentials and apparently accelerated inactivation kinetics in all channels. Moreover, flecainide slowed recovery from inactivation in all the channel complexes and suppressed the 'overshoot' in K_V4.3/KChIP2/MiRP1 channels.
Conclusions and implications: Flecainide directly binds to the K_V4.3 α-subunit when the channels are in the open and inactivated state and the presence of the β-subunits modulates the blockade by altering the gating function.
British Journal of Pharmacology (2008) **154,** 774–786; doi:10.1038/bjp.2008.134; published online 21 April 2008

Keywords: Flecainide; K_V4.3; MiRP1; DPP6; KChIP2; transient outward current; cardiac

Abbreviations: CHO, Chinese hamster ovary cells; DPP6, dipeptidyl-aminopeptidase-like protein 6; I_{to}, transient outward potassium current; KChIP2, K_V channel-interacting protein type 2; MiRP1, minK-related peptide 1

Introduction

Voltage-dependent K^+ channels are formed by channel pore-forming (α) and accessory (β) subunits (Roden *et al.*, 2002; Tamargo *et al.*, 2004; Nerbonne and Kass, 2005). The α-subunits are transmembrane proteins that assemble as tetramers, whereas the β-subunits represent a diverse molecular group that includes cytoplasmic and single transmembrane-spanning proteins. In the human heart, the Ca^{2+}-independent transient outward K^+ current (I_{to}) is critical in determining the height and the duration of the plateau phase of the action potential and is encoded by the K_V4.3 α-subunit (Dixon *et al.*, 1996). However, when this α-subunit is expressed in heterologous systems, the current obtained is similar to, but does not fully reproduce, native I_{to}, suggesting that β-subunits may play a significant role in the phenotype of the native current. Within these subunits, KChIP2 (Rosati *et al.*, 2001), the dipeptidyl-aminopeptidase-like protein 6 (DPP6) (Radicke *et al.*, 2005) and the KCNE2-encoded MinK-related peptide 1 (MiRP1) (Radicke *et al.*, 2006) have been proposed as likely candidates that coassemble with K_V4.3 in the human heart.

KChIP2 is a cytosolic Ca^{2+}-binding ancillary subunit that interacts with the amino terminus of the K_V4 α-subunit

Correspondence: R Gómez, Department of Pharmacology, School of Medicine, Universidad Complutense, 28040 Madrid, Spain.
E-mail: ricardo.gomez@med.ucm.es
[3]These authors contributed equally to this work.
Received 30 October 2007; revised 14 January 2008; accepted 13 March 2008; published online 21 April 2008

(An *et al*., 2000; Wang *et al*., 2007). KChIP2 modifies K_V4-encoded currents by increasing the current and surface channel density, slowing inactivation, accelerating recovery from inactivation and shifting the midpoint of the inactivation curve to depolarised potentials (An *et al*., 2000; Pourrier *et al*., 2003). DPP6 and MiRP1 are single membrane-spanning proteins that can influence channel gating through diverse mechanisms, which involve direct interactions with α-subunit transmembrane core domains, including the pore and the voltage-sensing domain (Dougherty and Covarrubias, 2006). DPP6 coexpression with K_V4.3 results in an acceleration of the activation and inactivation kinetics and a leftward shift of the midpoint of activation and inactivation curves (Nadal *et al*., 2003; Ren *et al*., 2005). Therefore, it has been proposed that DPP6 promotes activation and inactivation of K_V4 channels by mainly interacting with the voltage-sensing domain of the channel (Ren *et al*., 2005; Dougherty and Covarrubias, 2006). In contrast, MiRP1 slows the rates of K_V4 activation and inactivation (Zhang *et al*., 2001) and induces an 'overshoot' of the current amplitude during channel recovery from inactivation (Zhang *et al*., 2001; Radicke *et al*., 2006), a phenomenon previously observed with the I_{to} from human subepicardial myocytes (Wettwer *et al*., 1994). In fact, MiRP1 is thought to hinder both channel activation and inactivation processes by interacting with the pore domains of the channel (Zhang *et al*., 2001; Melman *et al*., 2004).

Although there is considerable information on the biophysical effects of β-subunits on K_V4 channels, much less is known about the effects of this interaction on the pharmacological response of these channels to drugs. Flecainide is a class IC antiarrhythmic drug, which also acts as an open and inactivated state blocker of I_{to} and K_V4 channels (Slawsky and Castle, 1994; Wang *et al*., 1995; Yeola and Snyders, 1997). Flecainide exhibits high affinity for K_V4.3 channels and, in fact, it has been used as a pharmacological tool to differentiate K_V4-generated flecainide-sensitive I_{to} from K_v1.4-generated flecainide-insensitive I_{to} (Yeola and Snyders, 1997). The high sensitivity has been attributed to a leucine residue located at the S6 transmembrane domain of K_V4.2 channels (L392), which is conserved in K_V4.3 channels (L393) (Herrera *et al*., 2005). Moreover, it has been suggested that the presence of KChIP2 does not modify the pharmacological sensitivity of K_V4 (Rosati *et al*., 2001).

The presence of auxiliary subunits that modify the activation and inactivation processes of channels can affect the channel blockade because conformational changes associated with gating can determine the access to and/or the affinity for the drug-binding site. A previous study has demonstrated that the presence of MiRP1 slows the unbinding rate of 4-aminopyridine from K_V4 channels, which, in contrast to most of the K^+ channel blockers, is a closed state blocker that binds to the inner mouth of K_V4 channels in the resting state and unbinds when channels open (Zhang *et al*., 2001). Therefore, this work was undertaken to test the effects of the presence of either DPP6 or MiRP1 on the flecainide-induced block of K_V4.3/KChIP2 channels, as each subunit exerts opposite effects on channel gating. Also, the effects of flecainide on K_V4.3 channels in the presence of both subunits were tested. The results suggest that flecainide directly binds to the K_V4.3 α-subunit and the affinity for the binding site is not modified by the presence of the different β-subunits. However, due to the different effects of β-subunits on current activation and inactivation kinetics, significant differences in drug effects on peak current amplitude and inactivated channels were observed.

Methods

Cell culture

Chinese hamster ovary (CHO) cells stably transfected with hK_V4.3-L/hKChIP2a (K_V4.3/KChIP2) were cultured as described previously (Radicke *et al*., 2005). The cells were transiently transfected with the cDNA encoding either MiRP1 (1 μg), DPP6 (1 μg) or both proteins (1 μg of each), together with the cDNA encoding the CD8 antigen (0.5 μg), using FuGENE 6 transfection reagent following the manufacturer's instructions. Before experimental use, cells were incubated with polystyrene microbeads precoated with anti-CD8 antibody. Most of the cells that were beaded had also channel expression (Caballero *et al*., 2004; Vaquero *et al*., 2007).

Recording techniques for ionic currents

Currents were recorded at room temperature (22 °C) using the whole-cell configuration of the patch-clamp technique with Axopatch 200B amplifiers and pCLAMP 9.0 software (Axon Instruments, Foster City, CA, USA) as described previously (Caballero *et al*., 2004; Vaquero *et al*., 2007). K_v4.3 currents were sampled at 4 kHz and filtered at 1 kHz. Pipettes were pulled from Narishige borosilicate capillary tubes using a programmable patch micropipette puller (P-2000) and were heat-polished with a microforge. Micropipette resistance was kept below 3.5 MΩ when filled with internal solution and immersed in external solution. Maximum K_V4.3 current amplitudes averaged 2.5 ± 0.5 nA ($n = 38$). No differences in maximum current amplitude and density were found among the channels studied. Access resistance and cell capacitance were 4.3 ± 0.6 MΩ and 15.7 ± 1.5 pF, respectively. Typically ≈80% of capacitance and series resistance were compensated for obtaining mean uncompensated access resistances of 1.9 ± 0.2 MΩ. Thus, no significant voltage errors (< 5 mV) due to micropipette series resistance were expected.

Pulse protocols and analysis

The holding potential was maintained at −80 mV and the cycle time for any protocol was 10 s to avoid accumulation of inactivation and/or block as previously described for K_V4.3 currents (Caballero *et al*., 2004; Radicke *et al*., 2006; Vaquero *et al*., 2007). The protocol used to obtain current–voltage relationships consisted of 250-ms pulses that were imposed in 10-mV steps between −90 and + 50 mV. The protocol used to obtain the activation curves consisted of a 5-ms conditioning pulse that was imposed in 10-mV increments between −80 and + 60 mV followed by a 200-ms pulse to −30 mV. To obtain steady-state inactivation curves, a

two-step protocol was used: the first 250-ms conditioning pulse from −80 mV to potentials between −90 and +50 mV was followed by a test pulse (250 ms) to +50 mV. Activation and inactivation curves were constructed by plotting the peak current amplitude obtained with the test pulse as a function of the voltage command of the conditioning pulse. The time course of recovery from inactivation was determined with a double-pulse protocol consisting of twin 500-ms pulses from a holding potential of −80 mV to +50 mV, separated by a recovery interval at −80 mV of variable duration (5–4000 ms). The ratio between the current amplitude obtained with the test pulse and the first pulse (I_{test}/I) was plotted as a function of the recovery interval duration. An exponential analysis was used to calculate the time constant of the recovery from the inactivation (Radicke *et al*., 2006).

To obtain the IC_{50} (concentration of drug that produces half maximum blockade) and the Hill's coefficient, n_H, a Hill's equation was fitted to the percentage of block (f) obtained at various drug concentrations [D]:

$$f = 1/\{1 + (IC_{50}/[D])^{n_H}\}$$

Once the concentration–response curve was obtained, a concentration close to the IC_{50} value was used to characterize the effects of flecainide on the channels.

To describe the time course of current activation and inactivation upon depolarization an exponential analysis was used.

Apparent rate constants for association (k) and dissociation (l) were obtained as previously described (Caballero *et al*., 2004) from fitting:

$$1/\tau_{Block} = k[D] + l$$

where τ_{Block} is the time constant of development of the fractional block (FB), which is determined as the ratio between the flecainide-sensitive current during the pulse to +50 mV and the current in control conditions ($FB = (I_C - I_F)/I_C$), and [D] is the concentration of drug.

Statistical methods

Data obtained in the absence and presence of flecainide were compared in a paired manner. For comparisons at a single voltage, differences were analysed by using Student's t-test. To analyse block at multiple voltages and differences between parameters of two different channels, a two-way ANOVA was used, followed by Newman–Keuls test. Results were expressed as mean ± s.e.m. $P<0.05$ was considered statistically significant.

Nomenclature of ion channels conforms with *BJP*'s Guide to Receptors and Channels (Alexander *et al*., 2007).

Solutions, drugs and materials

CHO cells were superfused with an external solution containing (mM): NaCl 136, KCl 4, $CaCl_2$ 1, $MgCl_2$ 1, HEPES 10 and glucose 10 (pH = 7.4 with NaOH). The internal solution contained (mM): K-aspartate 80, KCl 42, KH_2PO_4 10, MgATP 5, phosphocreatine 3, HEPES 5 and EGTA 5 (pH = 7.2 with KOH). Flecainide (Sigma, St Louis, MO, USA) was dissolved in methanol to yield 0.01 M stock solutions. Control solutions contained the same solvent concentration as the test solution.

FuGENE 6 transfection reagent was obtained from Roche Diagnostics (Mannheim, Germany); microbeads precoated with anti-CD8 antibody (Dynabeads M450) from Dynal, (Norway); Narishige borosilicate capillary tubes (GD1) and microforge (MF-83) from Narishige Co. Ltd. (Tokyo, Japan); micropipette puller (P-2000) from Sutter Instruments Co. (Novato, CA, USA).

Results

Effects of flecainide on $K_V4.3$ currents

Figures 1a–d show the effects of 20 μM flecainide on current traces generated by $K_V4.3$/KChIP2, $K_V4.3$/KChIP2/MiRP1 (+MiRP1), $K_V4.3$/KChIP2/DPP6 (+DPP6) and $K_V4.3$/KChIP2/MiRP1/DPP6 (+MiRP1+DPP6) channels after applying 250-ms pulses to +50 mV from a holding potential of −80 mV. At this concentration, flecainide reduced the peak current amplitude by 37.4 ± 4.1% ($n=12$), 47.2 ± 5.8% ($n=12$), 32.4 ± 6.1% ($n=8$) and 40.4 ± 4.9% ($n=6$) on $K_V4.3$/KChIP2, +MiRP1, +DPP6 and +MiRP1+DPP6 channels, respectively. The peak reduction on each channel was plotted as a function of the flecainide concentration and the concentration-dependence of the peak inhibition was calculated. The Hill's equation was fitted to each plot and the IC_{50} and n_H were calculated (Table 1). Interestingly, the peak IC_{50} value for +MiRP1 channels was significantly lower (20 μM), whereas those of +DPP6 and +MiRP1+DPP6 channels were significantly higher (142 μM and 57 μM, respectively), than that obtained for $K_V4.3$/KChIP2 (29 μM) (Table 1).

As can be seen from the current traces, flecainide accelerated the current decay in all combinations of channel subunits (see below). These actions of flecainide are suggestive of an open-channel block mechanism, in which case the reduction of peak current would not represent the steady-state block. Therefore, flecainide-induced block was also measured as the reduction of the total charge crossing the membrane (calculated as current–time integrals at +50 mV). Figures 1e–h show the concentration–response curves, obtained by plotting the reduction of total charge crossing the membrane at +50 mV as a function of flecainide concentration. As shown in Table 1, charge IC_{50} values (~10 μM) were not significantly different among the different channels studied. For all the channels, flecainide was more potent at decreasing the current–time integrals than the peak currents. This difference in IC_{50} values was smallest for +MiRP1.

To assess the onset of block, the FB, determined as the ratio between the flecainide-sensitive current during the pulse to +50 mV and the current in control conditions ($FB = (I_C - I_F)/I_C$), was calculated for all the concentrations tested. As observed in the examples shown in Figures 2a–d, the inhibitory effect of 20 μM flecainide began with the depolarising pulse and then increased until it reached a

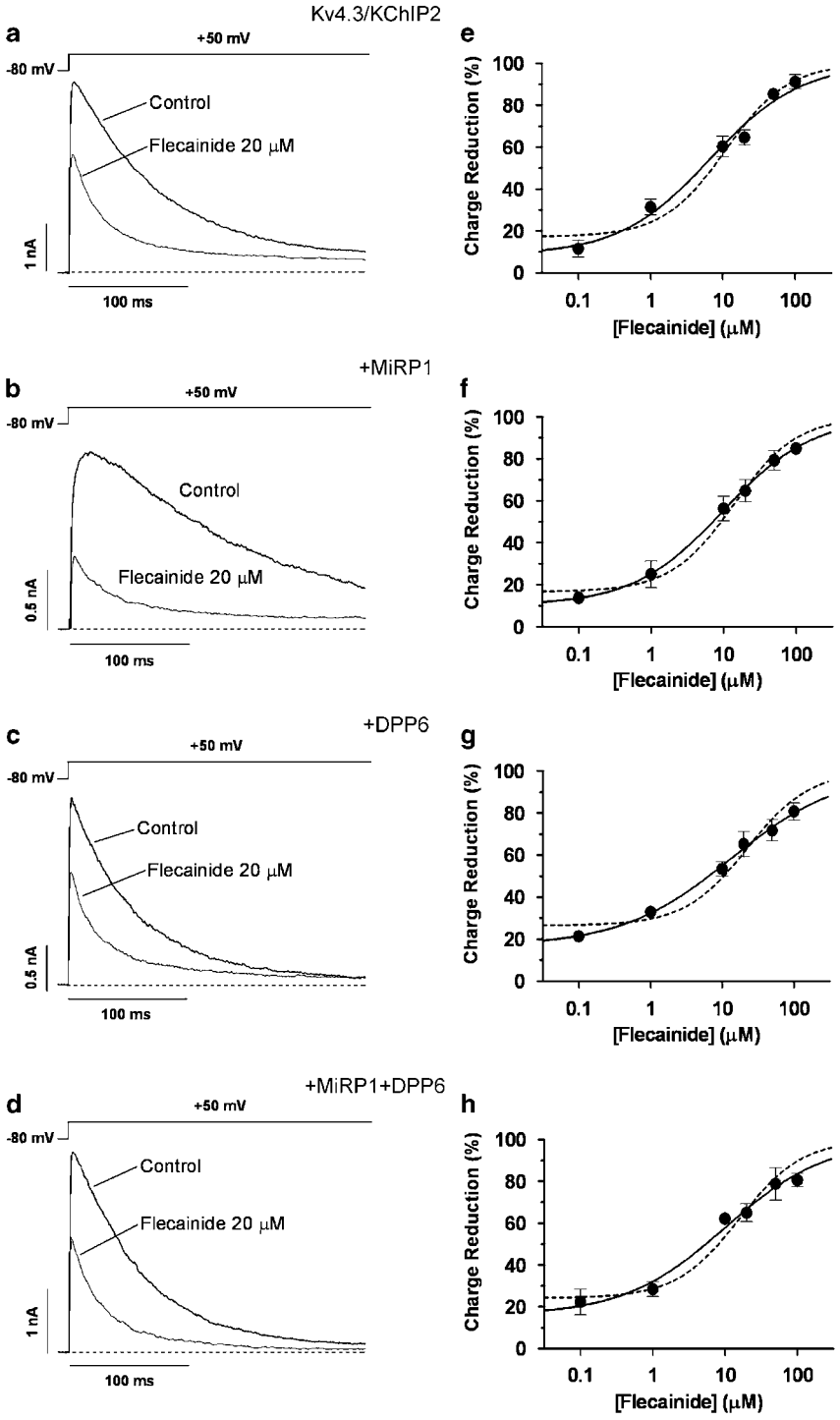

Figure 1 Effects of flecainide on K_V4.3 currents. (**a**–**d**) Representative current traces of K_V4.3/KChIP2 (**a**), +MiRP1 (**b**), +DPP6 (**c**) and +MiRP1+DPP6 (**d**) channels, recorded by applying 250 ms pulses from −80 to +50 mV in the absence and presence of 20 μM flecainide. Dotted lines represent the zero current level. (**e**–**h**) Reduction of total K_V4.3 charge crossing the membrane at +50 mV plotted as a function of flecainide concentrations. The Hill's equation was fitted to the data, the n_H was either fixed to unity (continuous line) or not (dashed line). Each data point represents the mean ± s.e.mean of >6 experiments.

steady-state level. To determine the τ_{Block}, a monoexponential function (continuous line) was fitted to the FB, averaging 11.8 ± 2.6 ms (n = 9), 5.9 ± 1.1 ms (n = 10), 8.8 ± 1.5 ms (n = 8) and 6.5 ± 1.3 ms (n = 6) for K_V4.3/KChIP2, +MiRP1, +DPP6 and +MiRP1+DPP6 channels, respectively. The plot of $1/\tau_{Block}$ as a function of flecainide concentration (0.1–100 μM) is presented in Figures 2e–h. The straight line is the least-squares fit, used to calculate the apparent association (k) and

Table 1 Concentration-dependent effects of flecainide on K_V4.3 currents

	IC_{50} (μM)			*Onset block kinetics*		
	Peak	*Charge*	*Inactivation*	K_d *(μM)*	k *($\mu M^{-1} s^{-1}$)*	l *(s^{-1})*
K_V4.3/KChIP2 ($n=18$)	29.1 ± 4.9	6.7 ± 1.0	10.8 ± 2.2	5.8	5.6 ± 0.6	32.8 ± 16.4
+ MiRP1 ($n=16$)	19.6 ± 2.0*	9.8 ± 0.4	9.7 ± 1.7	13.9	4.7 ± 0.1	65.6 ± 16.9
+ DPP6 ($n=16$)	142.1 ± 27.4*	13.2 ± 0.8	0.5 ± 0.1*	10.8	4.4 ± 0.5	47.2 ± 24.8
+ MiRP1 + DPP6 ($n=10$)	56.7 ± 3.9*	9.8 ± 1.5	2.9 ± 0.7*	11.9	4.0 ± 0.3	47.9 ± 12.2

Abbreviations: DPP6, dipeptidyl-aminopeptidase-like protein 6; IC_{50}, half maximum inhibitory concentration derived from concentration–response curves in which reduction in peak current, charge and peak current after 250-ms conditioning prepulses to −30 mV were used as an index of block; K_d, calculated equilibrium dissociation constant ($K_d = l/k$); MiRP1, minK-related peptide 1.
*$P<0.05$ vs K_V4.3/KChIP2 channels.

dissociation (l) rate constants, and, subsequently, the equilibrium dissociation constant ($K_d = l/k$) (Table 1). The K_d values calculated were similar to the charge IC_{50} values for all the channels (range 5.8–13.9 μM).

Effects of flecainide on the time to peak and on the time course of inactivation

As evident from the current traces shown in Figures 1a–d, one of the main differences between the channels studied was the activation and inactivation kinetics. With respect to the activation process, as the activation and inactivation partially overlap, we have restricted the analysis to the effects of flecainide on the time to peak. Figure 3a shows the differences in the times to peak of currents elicited by pulses to + 50 mV and the effects of flecainide on them. In control conditions, time to peak of K_V4.3/KChIP2 channels averaged 4.1 ± 0.3 ms ($n=8$). The presence of DPP6 alone or together with MiRP1 did not modify the current activation, whereas the presence of MiRP1 alone significantly slowed the activation process prolonging the time to peak (10.2 ± 1.7 ms, $n=9$, $P<0.05$). Figure 3b shows representative examples of K_V4.3/KChIP2, + MiRP1, + DPP6 and + MiRP1 + DPP6 currents normalised to the maximum amplitude to better compare the differences in activation kinetics. In all the channels studied, 20 μM flecainide shortened the time to peak in a significant manner (an example is given in Figure 3c), suggesting that it truncated the activation phase by binding to the open state of the channels.

The kinetics of the inactivation process of K_V4.3 channels was assessed by the biexponential fit to the decay of currents elicited by pulses to + 50 mV. As shown in Figures 4a and b, + MiRP1 channels had the slowest inactivation process, reflected by the highest fast ($\tau_{f,inact}$) and slow ($\tau_{s,inact}$) time constants of inactivation ($\tau_f = 55.3 \pm 12.0$ ms and $\tau_s = 245.4 \pm 55.4$ ms, $n=12$). On the other hand, the presence of DPP6 alone or together with MiRP1 accelerated the inactivation process, significantly decreasing the $\tau_{f,inact}$ ($P<0.05$ vs K_V4.3/KChIP2, Figure 4a). As we mentioned previously, flecainide (20 μM) produced a significant acceleration of the inactivation process, reducing both $\tau_{f,inact}$ and $\tau_{s,inact}$ on + MiRP1 and K_V4.3/KChIP2 channels, but only $\tau_{f,inact}$ on + DPP6 and + MiRP1 + DPP6 channels (Figures 4a and b). This acceleration of the inactivation kinetics was accompanied by an increase in the relative amplitude of the fast component (Figure 4c), and an equivalent decrease of the slow component (Figure 4d), of the inactivation.

Voltage-dependence of the flecainide-induced block

Figure 5a shows representative K_V4.3/KChIP2 current traces obtained in the absence and presence of 20 μM flecainide with the protocol shown at the top. Figures 5b–e show charge–voltage relationships in the absence and presence of 20 μM flecainide for K_V4.3/KChIP2, + MiRP1, + DPP6 and + MiRP1 + DPP6 channels, respectively. Flecainide significantly decreased the total K_V4.3/KChIP2 charge at potentials positive to −20 mV (61.0 ± 3.8% at + 50 mV, $P<0.01$, $n=12$, Figure 5b). In a similar way, flecainide decreased + MiRP1 (63.1 ± 2.5% at + 50 mV, $P<0.01$, $n=12$, Figure 5c), + DPP6 (60.8 ± 6.1% at + 50 mV, $P<0.05$, $n=8$, Figure 5d) and + MiRP1 + DPP6 (66.0 ± 6.5% at + 50 mV, $P<0.05$, $n=6$, Figure 5e) current–time integrals at potentials positive to −20 mV. To quantify the effects of the voltage on the drug–channel interaction, the relative charge (Q_F/Q_C) was plotted as a function of the membrane potential (Vaquero *et al.*, 2007). In the four types of channel, the blockade appeared in the voltage range coinciding with that of channel activation, remaining constant at more positive potentials in K_V4.3/KChIP2 (53.7 ± 6.0% at −10 mV, $P>0.05$ vs blockade at + 50 mV), + MiRP1 (54.2 ± 6.9% at −10 mV, $P>0.05$ vs blockade at + 50 mV) and + MiRP1 + DPP6 channels (68.3 ± 5.2% at −10 mV, $P>0.05$ vs blockade at + 50 mV) but showing a significant increase in + DPP6 channels (31.3 ± 9.1% at −10 mV, $P<0.01$ vs blockade at + 50 mV, Figure 5d).

Figures 6a–d show activation curves obtained by plotting the amplitude of the 200-ms pulse to −30 mV as a function of the voltage of the conditioning pulse in the absence and presence of 20 μM flecainide (see Methods and upper left panel in Figure 6). In control conditions, the activation curve for K_V4.3/KChIP2 yielded a V_h value of 13.1 ± 3.3 mV (Table 2). The results demonstrated that the presence of DPP6, alone or together with MiRP1, significantly shifted the activation curve to hyperpolarised potentials, whereas the presence of MiRP1 alone did not significantly modify the voltage dependence of activation. Flecainide (20 μM) significantly shifted the V_h to more negative potentials in all the channels, without modifying the slope values (Figures 6a–d and Table 2).

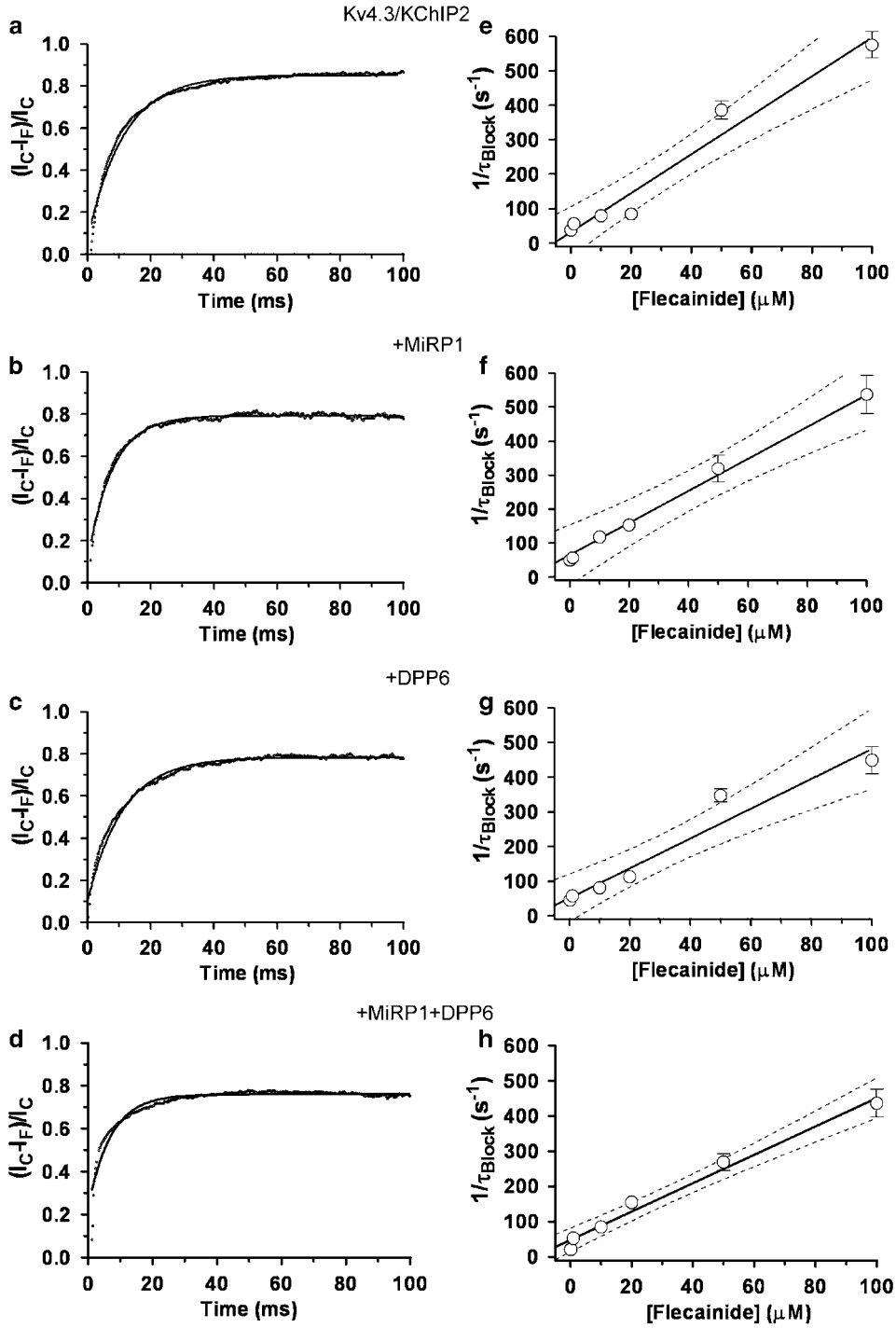

Figure 2 Analysis of the onset kinetics of the flecainide-induced block on K_V4.3/KChIP2, +MiRP1, +DPP6 and +MiRP1+DPP6 channels. (**a–d**) Ratio between the flecainide-sensitive current during pulses to +50 mV and the current in control conditions ($(I_C-I_F)/I_C$) in representative experiments. The continuous lines represent the monoexponential function fit to obtain the τ_{Block} at 20 μM flecainide. (**e–h**) $1/\tau_{Block}$ as a function of the flecainide concentrations tested. The straight line is the least-squares fit and the dotted line is the 95% confidence interval of the fit. Each data point represents the mean ± s.e.mean of ⩾6 experiments.

Figures 6e–h show the inactivation curves constructed by plotting the peak current amplitude of the test pulse to +50 mV as a function of the voltage of the conditioning pulse (see Methods and upper right panel in Figure 6). In control conditions, the Boltzmann fit to the inactivation curves yielded a V_h value of −18.2 ± 2.5 mV for K_V4.3/KChIP2 channels. As observed in the activation curves, addition of DPP6, alone or together with MiRP1, but not of MiRP1 alone, shifted the voltage dependence of inactivation to more negative potentials (Table 2). Again, there were no statistically significant differences between the slope values (Table 2). Flecainide significantly decreased the current

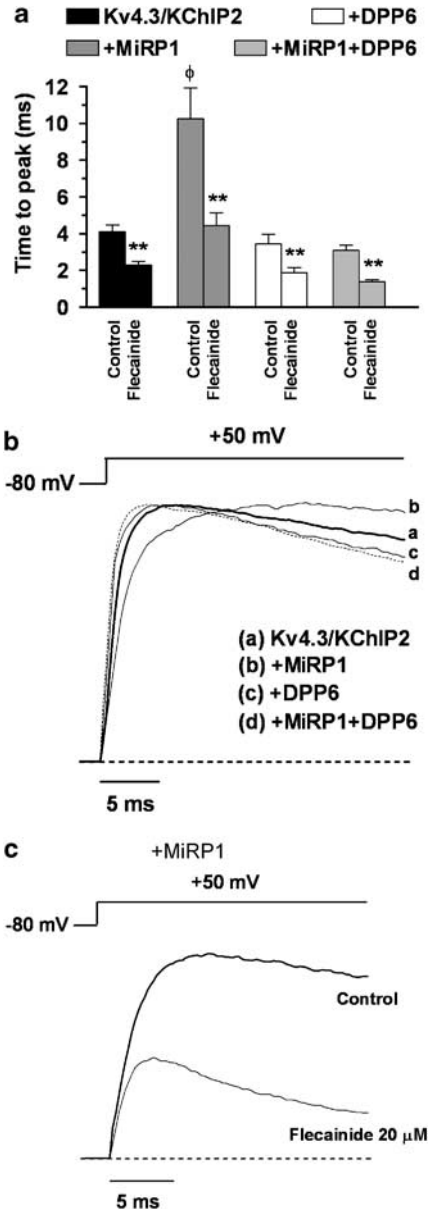

Figure 3 Effects of flecainide on time to peak current. (**a**) Time to peak values in control conditions and in the presence of 20 μM flecainide. Each column represents the mean ± s.e.mean. of ⩾7 experiments. (**b**) Normalised current traces recorded from K_V4.3/KChIP2, +MiRP1, +DPP6 and +MiRP1+DPP6 channels by applying pulses from −80 to +50 mV in control conditions. A representative current of each channel was shown. Dotted line represents the zero current level. (**c**) +MiRP1 current traces recorded by applying pulses from −80 to +50 mV in the absence and the presence of 20 μM flecainide. $^{**}P<0.01$ vs control. $^{\phi}P<0.05$ vs K_V4.3/KChIP2, +DPP6 and + MiRP1+DPP6.

amplitude at potentials negative to −20 mV and shifted the V_h to more negative potentials, without modification of the slope, in all the channels studied (Table 2). As observed from the representation of the relative current (represented as squares in Figures 6e–h), the flecainide-induced blockade slightly increased in the voltage range coinciding with that of channel inactivation, reaching statistical significance only for +DPP6 channels. The flecainide-induced inhibition after conditioning pulses to −30 mV was used as an index of the inactivated state block and plotted as a function of the flecainide concentrations. The IC_{50} values obtained using this index of block are summarised in Table 1. The results demonstrated that the lowest IC_{50} was that obtained for +DPP6 channels. Similar results were obtained with flecainide-induced inhibition after conditioning pulses to −20 mV was used as the index (data not shown).

Effects of flecainide on the time course of recovery from inactivation

The time course of recovery from inactivation was determined with a double-pulse protocol and fitted by an exponential function, as described in the Methods section. In control conditions, the time constants of the recovery process for K_V4.3/KChIP2 and +MiRP1+DPP6 channels were not significantly different (Figure 7a). However, of all the channel complexes, +DPP6 channels exhibited the fastest recovery kinetics. Interestingly, +MiRP1 channels presented the so-called 'overshoot', a phenomenon previously described for native human I_{to} recorded in epicardial ventricular myocytes (Wettwer *et al.*, 1994), K_V4.2 coexpressed with MiRP1 in Xenopus oocytes (Zhang *et al.*, 2001) and K_V4.3/KChIP2 coexpressed with MiRP1 in CHO cells (Radicke *et al.*, 2006). The 'overshoot' implies that, with recovery intervals up to 250 ms, peak current amplitude elicited by the test pulse was larger compared to that of the first pulse (Figure 7b). Therefore, a biexponential fit was needed to describe the recovery process of +MiRP1 channels (Figure 7c) and the time constant of the fast initial process was used for comparing +MiRP1 with the other channels ($\tau_{Cfast} = 76.7 \pm 18.9$ ms, $n=5$, $P>0.05$).

Flecainide (20 μM) slowed the recovery process on K_V4.3/KChIP2, +DPP6 and +MiRP1+DPP6 channels, increasing the time constants. However, in +MiRP1 channels, flecainide suppressed the observed 'overshoot', allowing the process to be described by a monoexponential fit ($\tau_F = 66.0 \pm 10.2$ ms, $P>0.05$ vs τ_{Cfast}) (Figure 7c).

Discussion

We analysed the effects of flecainide on K_V4.3/KChIP2 channels coassembled with MiRP1 and DPP6 β-subunits, which have been postulated as possible partners of K_V4.3 channels in native cells (Rosati *et al.*, 2001; Radicke *et al.*, 2005, 2006). The results demonstrate that the steady-state block produced by flecainide did not differ among the constructs. However, due to the different effects of β-subunits on current activation and inactivation kinetics, significant differences in drug effects on peak current amplitude and inactivated channels were observed.

Our data show that the coexpression of MiRP1 resulted in a significantly slower activation and inactivation compared to K_V4.3/KChIP2 channels. These results are in accordance with those obtained previously (Zhang *et al.*, 2001; Deschenes and Tomaselli, 2002). MiRP1 is known to be embedded within the channel in close proximity to or line part of the conduction pathway, interacting with or near to the S6 domain at the intracellular mouth region of the pore

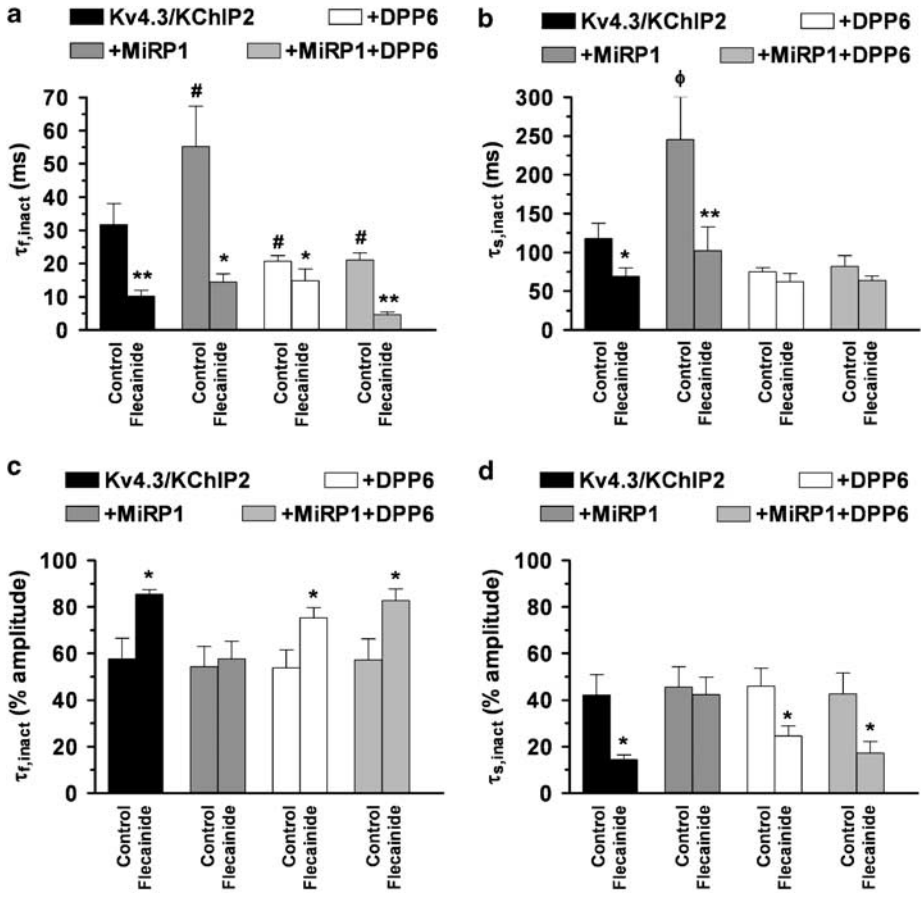

Figure 4 Effects of flecainide on time course of inactivation. (**a**, **b**) Time constants of inactivation ($\tau_{f,inact}$ and $\tau_{s,inact}$) in control conditions and in the presence of 20 μM flecainide. (**c**, **d**) Relative amplitudes of the fast and the slow components of the inactivation process in the absence and the presence of 20 μM flecainide. *$P<0.05$ vs control. **$P<0.01$ vs control. $^{\#}P<0.05$ vs $K_V4.3$/KChIP2. $^{\phi}P<0.05$ vs $K_V4.3$/KChIP2, + DPP6, and + MiRP1 + DPP6. Each column represents the mean ± s.e.mean of ⩾7 experiments.

(McCrossan and Abbott, 2004). Therefore, the interaction of MiRP1 with $K_V4.3$ could modify this region of the pore and, thus, hinder the conformational changes that are involved in both the activation and inactivation processes of K_V4 channels (Holmgren *et al*., 1998; Jerng *et al*., 1999; Zhang *et al*., 2001). The time course of the recovery from the inactivation was also modified. The + MiRP1 channels exhibited 'overshoot', a feature previously described when MiRP1 is coexpressed with $K_V4.3$ (Zhang *et al*., 2001). The 'overshoot' was not observed in the presence of other auxiliary subunits and is thought to demonstrate the involvement of MiRP1 in the formation of the channels that generate the human I_{to}, at least in left ventricular epicardial cardiomyocytes (Wettwer *et al*., 1994).

Our data also show that the coexpression of DPP6, alone or together with MiRP1, accelerates the current activation and inactivation processes compared to $K_V4.3$/KChIP2 channels. Again, these results confirm data described previously (Radicke *et al*., 2005; Ren *et al*., 2005; Dougherty and Covarrubias, 2006). Recent studies have indicated that coassembly of DPP6 produces a functional remodelling of K_V4 channels that depends on interactions involving the single membrane-spanning domain of DPP6 and certain residues in the S1 and S2 transmembrane segments of K_V4 channels (Ren *et al*., 2005; Dougherty and Covarrubias, 2006). Therefore, the DPP6-dependent remodelling may act to promote voltage-dependent activation and indirectly accelerate the coupled inactivation, and thus, the transition to the inactivated state (Dougherty and Covarrubias, 2006). Moreover, the significant shift of the midpoint of the activation and inactivation curves to hyperpolarised potentials could also be a result of the promotion of the activation. Nevertheless, it has to be considered that the present experiments were done at room temperature for a better control of the membrane potential during the fast current activation. This could limit the physiological relevance of the data, since temperature influences the gating characteristics of the channels and, consequently, the effects of the β-subunits.

To our knowledge, this is the first study in which the effects of the combined presence of MiRP1 and DPP6 were analysed. Our results demonstrated that, when both subunits are present, the time- and voltage-dependent properties of the channels were not different from those of + DPP6 channels. Indeed, the promotion of both activation and inactivation was apparent in these channels even when MiRP1 was present.

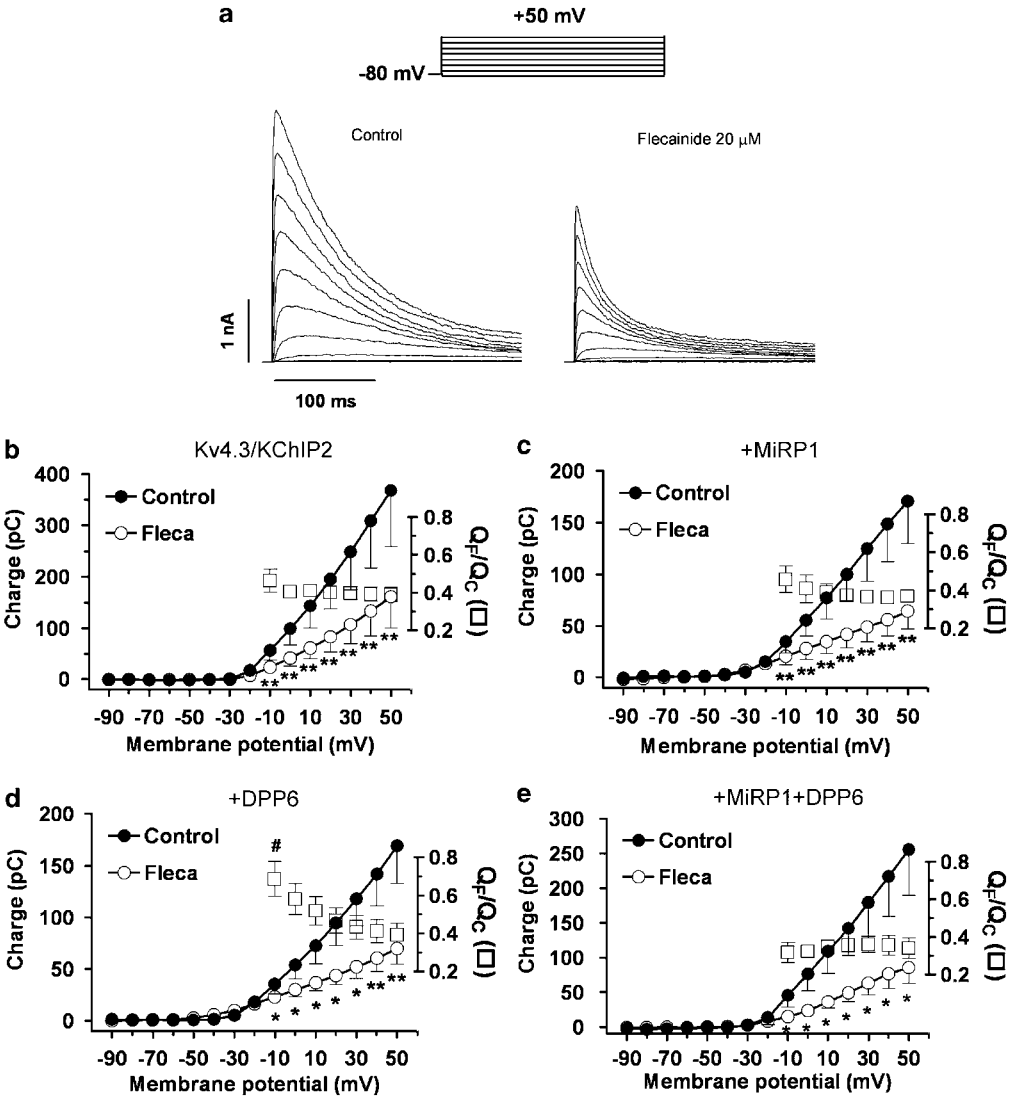

Figure 5 Charge-voltage relationships for K_V4.3/KChIP2, +MiRP1, +DPP6, and +MiRP1+DPP6 channels. (**a**) Representative K_V4.3/KChIP2 current traces in the absence and presence of 20 μM flecainide obtained when applying 250 ms pulses to potentials ranging from −90 to +50 mV. (**b**–**e**) Mean charge-voltage relationships in the absence and presence of 20 μM flecainide. The squares represent the ratio between the charge crossing the membrane in the presence and absence of flecainide (Q_F/Q_C) as a function of the membrane potential. *$P<0.05$ vs control. **$P<0.01$ vs control. $^{\#}P<0.05$ vs value at +50 mV. Each point represents the mean ± s.e.mean of ⩾6 experiments.

The IC_{50} values reflect the small modulation produced by the β-subunits on the flecainide-induced block

Flecainide produced similar qualitative effects in all the channels, that is, it inhibited the currents in a concentration-dependent manner, apparently accelerated the inactivation process, and produced a leftward shift of the midpoints of both the activation and inactivation curves. Moreover, the IC_{50} values obtained, when the total current charge (steady-state block) was analysed, were similar in the four channel complexes and similar to those obtained previously for K_V4.3 channels expressed in CHO cells (8 μM) (Singarayar *et al*., 2003) and in I_{to} registered in human atrial myocytes (≈10 μM) (Wang *et al*., 1995). Similar β-subunit-independent effects were also demonstrated for flecainide on canine endocardial and epicardial ventricular myocytes, which presented a different distribution of the KChIP2 subunit (Rosati *et al*., 2001), and for quinidine, E-4031 and dofetilide on K_V11.1 channels, with and without the coexpression of MiRP1 (Weerapura *et al*., 2002). These results indicate a direct interaction of flecainide with the pore-forming K_V4.3 protein, which is probably determined by the presence of leucine 393. This residue corresponds to leucine 392 of K_V4.2 channels, which has been implicated in their flecainide sensitivity (Herrera *et al*., 2005).

The apparent acceleration of the inactivation kinetics produced by flecainide was previously demonstrated in human atrial I_{to} and K_V4 channels (Wang *et al*., 1995; Yeola and Snyders, 1997) and has classically been attributed to a rapid open channel block. Since at the peak the number of open channels is at a maximum and the number of closed and inactivated channels is negligible, the peak IC_{50} value could be considered to represent the flecainide affinity for the open state of each channel. Moreover, the analysis of the development of block also demonstrated that there was no

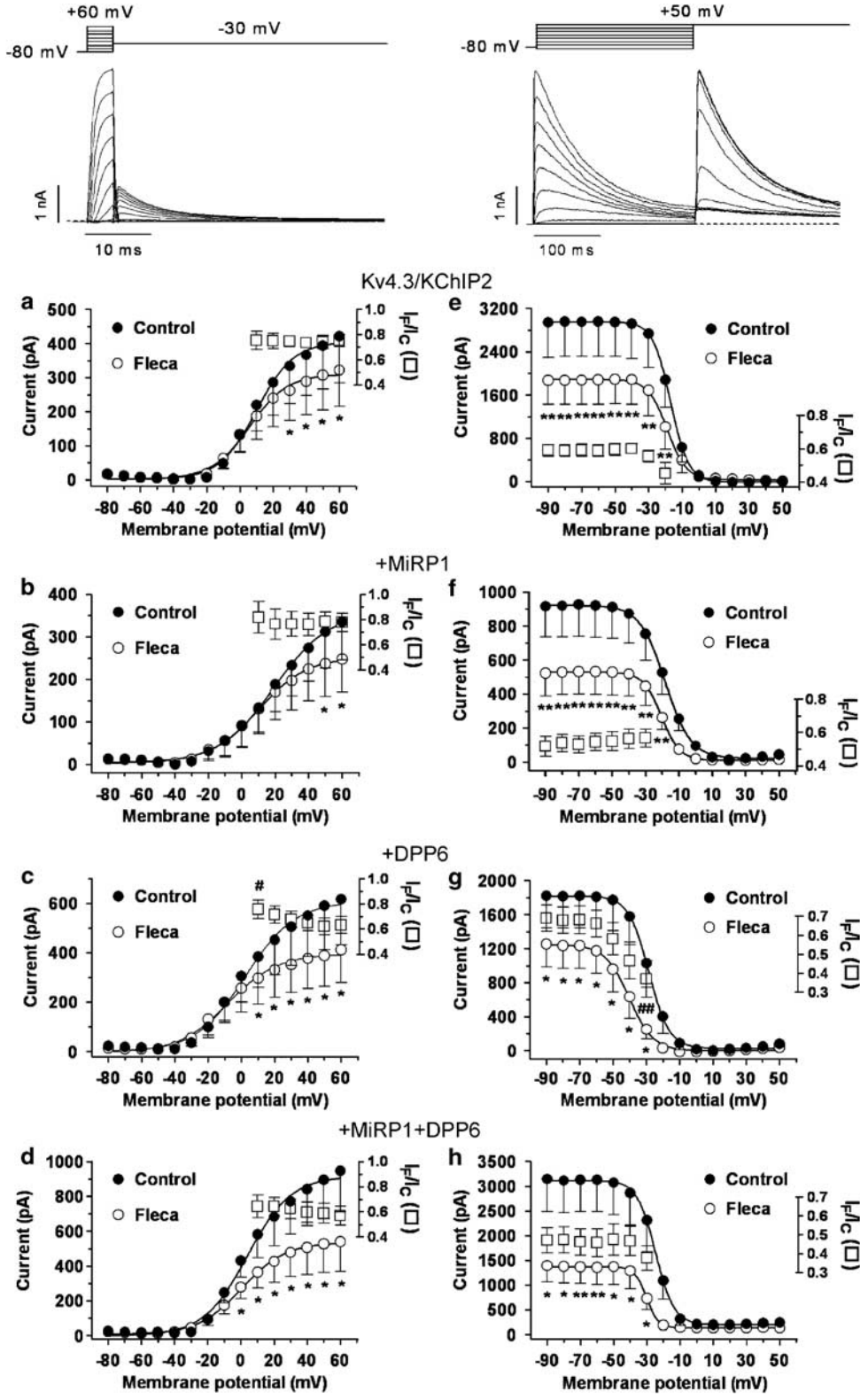

Figure 6 Voltage-dependence of the effects of flecainide on K_V4.3/KChIP2, + MiRP1, + DPP6, and + MiRP1 + DPP6 channels. Upper part shows the voltage protocols used for the analysis of the activation (left) and inactivation (right) processes of the channels and representative currents obtained in K_V4.3/KChIP2 channels. (**a**–**d**) Activation curves in the absence and presence of 20 μM flecainide. (**e**–**h**) Inactivation curves in the absence and presence of 20 μM flecainide. The squares represent the ratio between the current in the presence and absence of flecainide (I_F/I_C) as a function of the membrane potential. *$P<0.05$ vs control. **$P<0.01$ vs control. $^{\#}P<0.05$ vs value at + 60 mV. $^{\#\#}P<0.05$ vs value at −90 mV. Each point represents the mean ± s.e.mean of ⩾6 experiments.

Table 2 Voltage-dependent effects of flecainide on K_V4.3 channels activation and inactivation

	Voltage-dependence of activation			
	V_h (mV)		*Slope (mV)*	
	Control	*Flecainide*	*Control*	*Flecainide*
K_V4.3/KChIP2 ($n=11$)	13.1 ± 3.3	1.6 ± 3.7*	11.1 ± 0.7	9.7 ± 0.4
+ MiRP1 ($n=7$)	19.0 ± 4.8	12.4 ± 5.5*	13.5 ± 0.9	11.9 ± 1.4
+ DPP6 ($n=8$)	2.2 ± 3.3$^{\#}$	−9.5 ± 4.4**	11.2 ± 1.9	10.6 ± 1.2
+ MiRP1 + DPP6 ($n=6$)	2.0 ± 1.6$^{\#}$	−7.7 ± 3.9*	13.6 ± 2.4	11.2 ± 2.1
	Voltage-dependence of inactivation			
	V_h (mV)		*Slope (mV)*	
	Control	*Flecainide*	*Control*	*Flecainide*
K_V4.3/KChIP2 ($n=9$)	−18.2 ± 2.5	−22.1 ± 3.2*	4.9 ± 0.6	3.8 ± 0.6
+ MiRP1 ($n=11$)	−15.0 ± 1.9	−20.0 ± 2.1**	6.4 ± 0.6	4.9 ± 1.0
+ DPP6 ($n=7$)	−27.3 ± 2.0$^{\#}$	−36.7 ± 4.6*	5.2 ± 0.2	4.1 ± 0.3
+ MiRP1 + DPP6 ($n=6$)	−28.2 ± 1.9$^{\#}$	−31.7 ± 2.1*	4.4 ± 0.5	3.5 ± 0.4

Abbreviations: DPP6, dipeptidyl-aminopeptidase-like protein 6; MiRP1, minK-related peptide 1.
*$P<0.05$ vs control.
**$P<0.01$ vs control.
$^{\#}P<0.05$ vs K_V4.3/KChIP2 and + MiRP1 channels.

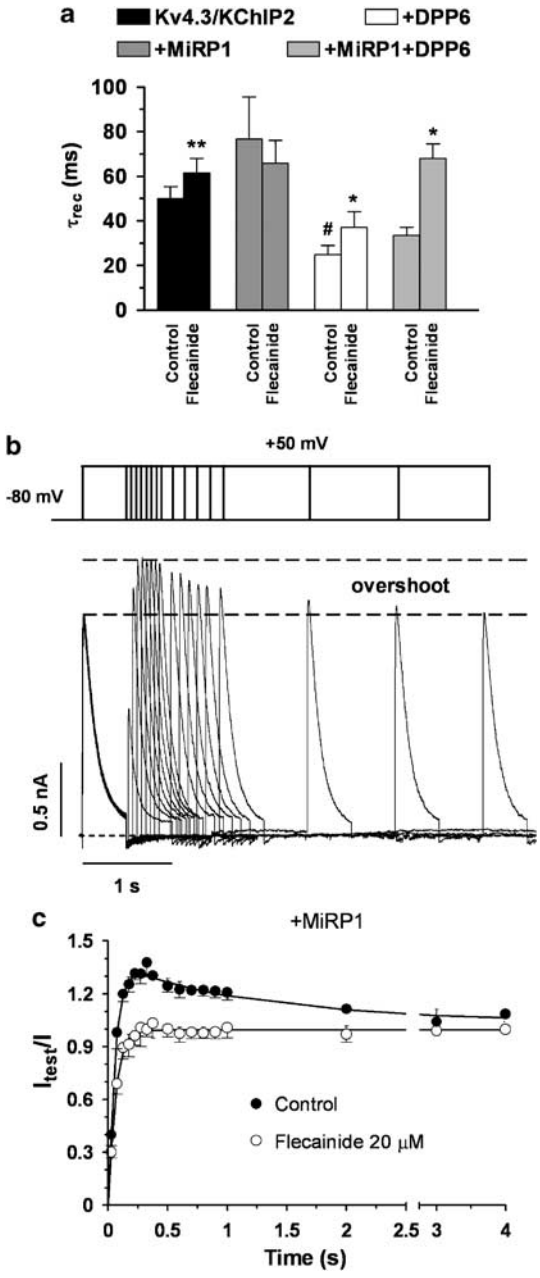

Figure 7 Effects of flecainide on time course of recovery from inactivation. (**a**) Time constants of recovery from inactivation (τ_{rec}) in control conditions and in the presence of 20 μM flecainide. (**b**) Representative + MiRP1 current traces during recovery from inactivation at −80 mV. (**c**) Time course of recovery from inactivation of + MiRP1, in control conditions and in the presence of 20 μM flecainide. Continuous lines represent the best fit to an exponential function. *$P<0.05$ vs control. **$P<0.01$ vs control. $^{\#}P<0.05$ vs K_V4.3/KChIP2. Each column or point represents the mean ± s.e.mean of ⩾5 experiments.

block before the application of the depolarising pulse, indicating that the blockade of the rested state is negligible. However, the IC_{50} values for peak current inhibition varied by a factor of seven between different channel complexes, which can easily be explained by the different effects of the subunits on K_V4.3 channel activation. As expected, the lowest peak IC_{50} was obtained for + MiRP1 channels, reflecting that the slow opening allows the development of block closer to a quasi steady-state block. In contrast, in the channels in which DPP6 was present, the peak IC_{50} was higher, as the fast activation/inactivation process hinders the development of open state block.

On the other hand, when a test pulse to + 50 mV is applied after a 250-ms conditioning pulse to −30 mV (and also to −20 mV), more of the K_V4.3 channels are in the inactivated state, and thus, the IC_{50} value calculated using the flecainide-induced inhibition at this potential as an index of block, in part, reflects the flecainide binding to the inactivated state. The lowest IC_{50} corresponded to + DPP6 channels, due to the marked acceleration of the transition to the inactivated state produced by DPP6, which allows a better saturation of binding of flecainide to the inactivated state. Overall, our results suggest that the presence of the β-subunits does not dramatically modify the topology of the flecainide-binding site in the K_V4.3 proteins and, thus, does not affect the affinity of this drug. Moreover, since the steady-state block reached was identical for all the channel complexes, our results also suggest that flecainide exhibits the same affinity for the channels when they are in the open and in the inactivated state. Indeed, the only requirement for blockade was that the channels were not in the resting state. However, since the effects of MiRP1 and DPP6 on I_{to} kinetics differed considerably, the effect of flecainide in native cells may vary depending on the composition of the complex, that is, an I_{to} with slow activation kinetics (MiRP1) should lead to a more pronounced inhibition of peak I_{to}. The significant binding of flecainide to the inactivated state probably determines the frequency dependence of current block, which may be more marked if DPP6 is part of the I_{to} channel complex.

Effects of flecainide on the voltage dependence of K_V4.3 channels
The significant leftward shift in the midpoint of the activation and the inactivation curves produced by flecainide, independently of the β-subunits coexpressed with K_V4.3, supports the aforementioned idea of an interaction of flecainide with both the open and the inactivated state of the channel.

In human atrial I_{to} (Wang *et al*., 1995) and in K_V4.3 channels coassembled with DPP6 (Figure 6 in this paper), the flecainide-induced block was voltage-dependent, the blockade increasing at membrane potentials at which channel activation and inactivation reached saturation. In contrast, on K_V4.3 alone (Singarayar *et al*., 2003), or coassembled with KChIP2, KChIP2 + MiRP1, and KChIP2 + MiRP1 + DPP6 (Figure 6 in this paper), the flecainide-induced block was not voltage-dependent. In K_v4.2 channels two valine residues (V402 and V404), that determined the intracellular binding of 4-aminopyridine, are also responsible for the voltage-dependent response to flecainide (Caballero *et al*., 2003). These valines, present in the deep intracellular S6 segment, are conserved in K_V4.3 channels (V399 and V401). It has been proposed that MiRP1, but not DPP6, interacts with the intracellular mouth of the K_V4.3 channel. Therefore, one possible explanation for the abolition of the voltage dependence of the flecainide-induced block when MiRP1 is present (either alone or combined with DPP6) could be that MiRP1 impedes the interaction of flecainide with these residues. In fact, it has been previously demonstrated that the presence of MiRP1 hinders the unbinding of 4-aminopyridine from the intracellular mouth of K_V4.2 channels (Zhang *et al*., 2001).

Conclusions
Flecainide blocked K_V4.3 channels in the open and inactivated state in a concentration-dependent manner and with a similar potency, and this effect was not dependent on the modulatory β-subunits (MiRP1 and/or DPP6) that coassembled with the K_V4.3/KChIP2 channels. The drug directly binds to the K_V4.3 α-subunit and the affinity for the binding site is not modified by the presence of the different β-subunits. However, due to the different effects of β-subunits on I_{to} activation and inactivation kinetics, the effects of flecainide may vary considerably depending on the I_{to}-complex composition in native cells.

Acknowledgements

We thank Guadalupe Pablo for her excellent technical assistance. We also thank Professor K Wada (National Institute of Neuroscience, Tokio, Japan) and Dr K Steinmeyer (Sanofi-Aventis Pharma, Frankfurt, Germany) for the DPP6 clone and transgenic CHO cells, respectively. This work was supported by grants from Comisión Interministerial de Ciencia y Tecnología (SAF2005-04609), Ministerio de Sanidad y Consumo, Instituto de Salud Carlos III (Red HERACLES RD06/0009), Sociedad Española de Cardiología and Lilly Foundation. SR was supported by the Dresdner Herz-Kreislauftage e.V. research award. RG was a fellow of the Comunidad Autónoma de Madrid.

Conflict of interest

The authors state no conflict of interest.

References

Alexander SPH, Mathie A, Peters JA (2007). Guide to Receptors and Channels (GRAC), 2nd edition (2007 revision). *Br J Pharmacol* **150** (Suppl 1): S1–S168.

An WF, Bowlby MR, Betty M, Cao J, Ling HP, Mendoza G *et al*. (2000). Modulation of A-type potassium channels by a family of calcium sensors. *Nature* **403**: 553–556.

Caballero R, Gómez R, Núñez L, Moreno I, Tamargo J, Delpón E (2004). Diltiazem inhibits hKv1.5 and Kv4.3 currents at therapeutic concentrations. *Cardiovasc Res* **64**: 457–466.

Caballero R, Pourrier M, Schram G, Delpón E, Tamargo J, Nattel S (2003). Effects of flecainide and quinidine on Kv4.2 currents: voltage dependence and role of S6 valines. *Br J Pharmacol* **138**: 1475–1484.

Deschenes I, Tomaselli GF (2002). Modulation of Kv4.3 current by accessory subunits. *FEBS Letters* **528**: 183–188.

Dixon JE, Shi W, Wang HS, McDonald C, Yu H, Wymore RS *et al*. (1996). Role of the Kv4.3 K^+ channel in ventricular muscle. A molecular correlate for the transient outward current. *Circ Res* **78**: 659–668.

Dougherty K, Covarrubias M (2006). A dipeptidyl aminopeptidase-like protein remodels gating charge dynamics in Kv4.2 channels. *J Gen Physiol* **128**: 745–753.

Herrera D, Mamarbachi A, Simoes M, Parent L, Sauvé R, Wang Z *et al*. (2005). A single residue in the S6 transmembrane domain governs the differential flecainide sensitivity of voltage-gated potassium channels. *Mol Pharmacol* **68**: 305–316.

Holmgren M, Shin KS, Yellen G (1998). The activation gate of a voltage-gated K^+ channel can be trapped in the open state by an intersubunit metal bridge. *Neuron* **21**: 617–621.

Jerng HH, Shahiduliah M, Covarrubias M (1999). Inactivation gating of Kv4 potassium channels: molecular interactions involving the inner vestibule of the pore. *J Gen Physiol* **113**: 641–659.

McCrossan ZA, Abbott GW (2004). The MinK-related peptides. *Neuropharmacology* **47**: 787–821.

Melman YF, Um SY, Krumerman A, Kagan A, McDonald TV (2004). KCNE1 binds to the KCNQ1 pore to regulate potassium channel activity. *Neuron* **42**: 927–937.

Nadal MS, Ozaita A, Amarillo Y, de Miera EV, Ma Y, Mo W *et al*. (2003). The CD26-related dipeptidyl aminopeptidase-like protein DPPX is a critical component of neuronal A-type K^+ channels. *Neuron* **37**: 449–461.

Nerbonne JM, Kass RS (2005). Molecular physiology of cardiac repolarization. *Physiol Rev* **85**: 1205–1253.

Pourrier M, Schram G, Nattel S (2003). Properties, expression and potential roles of cardiac K^+ channel accessory subunits: MinK, MiRPs, KChIP and KChAP. *J Memb Biol* **194**: 141–152.

Radicke S, Cotella D, Graf EM, Banse U, Jost N, Varró A *et al*. (2006). Functional modulation of the transient outward current Ito by KCNE β-subunits and regional distribution in human non-failing and failing hearts. *Cardiovasc Res* **71**: 695–703.

Radicke S, Cotella D, Graf EM, Ravens U, Wettwer E (2005). Expression and function of dipeptidyl-aminopeptidase-like protein 6 as a putative β-subunit of human cardiac transient outward current encoded by Kv4.3. *J Physiol* **565**: 751–756.

Ren X, Hayashi Y, Yoshimura N, Takimoto K (2005). Transmembrane interaction mediates complex formation between peptidase homologues and Kv4 channels. *Mol Cell Neurosci* **29**: 320–332.

Roden DM, Balser JR, George AL, Anderson ME (2002). Cardiac ion channels. *Annu Rev Physiol* **64**: 431–475.

Rosati B, Pan Z, Lypen S, Wang HS, Cohen I, Dixon JE *et al*. (2001). Regulation of KChIP2 potassium channel β subunit gene expression

underlies the gradient of transient outward current in canine and human ventricle. *J Physiol* **533**: 119–125.

Singarayar S, Bursill J, Wyse K, Bauskin A, Wu W, Vanderberg J *et al*. (2003). Extracellular acidosis modulates drug block of Kv4.3 currents by flecainide and quinidine. *J Cardiovasc Electrophysiol* **14**: 641–650.

Slawsky MT, Castle NA (1994). K+ channel blocking actions of flecainide compared with those of propafenone and quinidine in adult rat ventricular myocytes. *J Pharmacol Exp Ther* **269**: 66–74.

Tamargo J, Caballero R, Gómez R, Valenzuela C, Delpón E (2004). Pharmacology of cardiac potassium channels. *Cardiovasc Res* **62**: 9–33.

Vaquero M, Caballero R, Gómez R, Núñez L, Tamargo J, Delpón E (2007). Effects of atorvastatin and simvastatin on atrial plateau currents. *J Mol Cell Cardiol* **42**: 931–945.

Wang H, Yan Y, Liu Q, Huang Y, Shen Y, Chen L *et al*. (2007). Structural basis for modulation of Kv4 K^+ channels by auxiliary KChIP subunits. *Nat Neurosci* **10**: 32–39.

Wang Z, Fermini B, Nattel S (1995). Effects of flecainide, quinidine, and 4-aminopyridine on transient outward and ultrarapid delayed rectifier currents in human atrial myocytes. *J Pharmacol Exp Ther* **272**: 185–196.

Weerapura M, Nattel S, Chartier D, Caballero R, Hébert TE (2002). A comparison of currents carried by HERG, with and without coexpression of MiRP1, and the native rapid delayed rectifier current. Is MiRP1 the missing link? *J Physiol* **540**: 15–27.

Wettwer E, Amos GJ, Posival H, Ravens U (1994). Transient outward current in human ventricular myocytes of subepicardial and subendocardial origin. *Circ Res* **75**: 473–482.

Yeola SW, Snyders DJ (1997). Electrophysiological and pharmacological correspondence between Kv4.2 current and rat cardiac transient outward curent. *Cardiovasc Res* **33**: 540–547.

Zhang M, Jiang M, Tseng GN (2001). MinK-related pepide 1 associates with Kv4.2 and modulates its gating function. Potential role as β subunit of cardiac transient outward channel? *Circ Res* **88**: 1012–1019.